Talanta 207 (2020) 120258

Contents lists available at ScienceDirect

Talanta

journal homepage: www.elsevier.com/locate/talanta

Autocatalytic DNA circuit for Hg^{2+} detection with high sensitivity and selectivity based on exonuclease III and G-quadruplex DNAzyme

Danhua Zhou[a,b,1], Lingwen Zeng[a,1], Jiafeng Pan[b], Qiong Li[b], Junhua Chen[b,*]

[a] School of Food Science and Engineering, Foshan University, Foshan, 528000, China
[b] Guangdong Key Laboratory of Integrated Agro-environmental Pollution Control and Management, Guangdong Institute of Eco-environmental Science & Technology, Guangzhou, 510650, China

ARTICLE INFO

Keywords:
Hg^{2+}
G-quadruplex
Label-free
Signal amplification
Biosensor

ABSTRACT

Utilizing G-quadruplex as the signal report probe, an ultrasensitive and label-free autocatalytic DNA circuit for Hg^{2+} detection on the basis of exonuclease III (Exo III)-assisted cascade signal amplification has been proposed. In the absence of Hg^{2+}, the hairpin A and the DNA1 cannot hybridize due to the thymine-thymine (T-T) mismatches. Therefore, hairpin probes with the 3′-protruding terminus can be resistant to Exo III digestion, preventing the G-rich sequence to be released. In the presence of Hg^{2+}, the combination of the DNA1 with the 3′ end-extruding hairpin A *via* T-Hg^{2+}-T coordination chemistry triggers the digestion reaction of Exo III, leading to the release of the DNA1 and the sequence with domains c, d, and e. Both of the DNA1 and the sequence with domains c, d, and e can combine with other hairpin probes and activate another round of the cleavage reaction. The produced G-rich sequence can form G-quadruplex structure by binding with *N*-Methyl mesoporphyrin IX (NMM). The biosensor exhibits excellent selectivity and high sensitivity for Hg^{2+}. The linear range of this biosensor is from 10 fM to 100 nM, and the linear equation can be expressed as: $F_{610} = 1.3 \times 10^5$ Lg C + 7.40×10^4 ($R^2 = 0.998$), in which F_{610} is the fluorescence intensity at 610 nm, C represents the Hg^{2+} concentrations, and Lg is the logarithm of 10. The detection limit is 10 fM. The biosensor is robust and can be applied to the detection of Hg^{2+} in water samples. By substituting the target-recognition elements, this sensing system can also be used for the detection of other metal ions.

1. Introduction

Hg^{2+} is regarded as one of the most dangerous metal ions in the environment, which causes severe damage to food safety and human health even at low concentrations [1,2]. Therefore, it has aroused wide attention in the design of new strategies to monitor Hg^{2+} in environmental samples. Several classical Hg^{2+} detection methods have been proposed, including atomic spectrometry [3] and inductively coupled plasma mass spectrometry [4]. However, those methods require complicated and expensive instrumentation and cumbersome laboratory analysis procedures. It has been recognized that Hg^{2+} can specifically bind to the thymine (T) residues to form a T-Hg^{2+}-T complex, which is even more stable than the A-T base pair [5]. In recent years, many methods have been developed for detecting Hg^{2+} on the basis of T-Hg^{2+}-T interactions [6–9], such as colorimetric chemosensors [10,11], which display instrument-free format and naked-eye readout. However, the colorimetric sensor usually suffers from low sensitivity. Therefore, it is quite essential to develop a new biosensor with simplified operation for Hg^{2+} detection with an amplified signal to meet the requirement of the maximum allowable level of Hg^{2+} in drinking water of 10 nM, a standard set by the U.S. Environmental Protection Agency (EPA).

An essential and efficient way to obtain an ultrasensitive biosensor is adopting a signal amplification strategy. Because of its exponential signal amplification capacity, DNA recycling amplification strategies has now become important tools for developing a variety of ultrasensitive sensors by using nucleic acid probes or aptamers as recognition components [12]. Most of ultrasensitive detectors depend on amplification labels (e.g., nanoparticles) [13], which requires intricate synthetic processes and multiple operation steps. Catalytic amplifiers, logic cascades, and autonomous molecular motors driven by toehold-mediated DNA strand displacement reaction [14,15] is another signal amplification method, however, it takes a long time to react, which is not conducive for practical applications. As a kind of sequence independent enzyme, since no specific recognition sequences were

* Corresponding author.
E-mail address: 222chenjunhua@163.com (J. Chen).
[1] The two authors contributed equally to this work.

https://doi.org/10.1016/j.talanta.2019.120258
Received 25 March 2019; Received in revised form 12 August 2019; Accepted 14 August 2019
Available online 14 August 2019
0039-9140/

required, Exo III-assisted signal amplification strategy exhibited distinctive advantages, such as short assay time and ease of use, which makes it more suitable for constructing universal biosensor platforms [16]. Exo III can catalyze the stepwise removal of mononucleotides from 3′-hydroxyl terminus of double-stranded DNA with a blunt or recessed 3′ terminus in a short period of time [17,18]. Moreover, it shows limited activity on single-stranded DNA and duplex DNA with a protruding 3′ end [19]. Exo III provides a more versatile sensing media for the amplified detection of DNA [20,21], proteins [22,23], and metal ions [24,25]. Thus, Exo III was utilized for the detection of Hg^{2+} in this study.

The G-quadruplex is a unique higher-order structure consisting of square-planar arrangements of guanine nucleobases stabilized by Hoogsteen hydrogen bonding and monovalent cations [26]. As an excellent signal reporter, it is formed by G-rich sequences generally stabilized by alkali metal cations, especially K^+ [27]. G-quadruplex is polymorphic, which can be used to design biosensors [28] and DNA-based architectures [29]. *N*-Methyl mesoporphyrin IX (NMM), an anionic porphyrin emitting weakly fluorescent signals, is characterized by a pronounced structural selectivity for G-quadruplexes other than duplexes, triplexes, or single-stranded forms. When NMM binds with G-quadruplexe, it exhibits significant enhancement in fluorescence [30,31]. In this study, a sensing platform for Hg^{2+} detection was constructed, which was based on Exo III-assisted signal amplification using caged G-quadruplex as the signal transducer.

2. Experimental

2.1. Materials and reagents

Exo III was purchased from New England Biolabs (Ipswich, MA). Dimethyl sulfoxide (DMSO), and tris-(hydroxymethyl) aminomethane (Tris) were obtained from Sigma-Aldrich (St. Louis,Mo). *N*-methyl mesoporphyrin IX (NMM) was purchased from Frontier Scientific Inc. (Logan, Utah, USA). 5 mM NMM stock solution was stored at −20 °C after being dissolved in DMSO. Other reagents and chemicals were of analytical grade and used without purification. All solution was prepared with ultrapure water (18.2 MΩ/cm) from a Millipore Milli-Qwater purification system (Billerica, MA).

All DNA oligonucleotides were ULTRAPAGE-purified and purchased from Shanghai SangonBiotechnology Co., Ltd. (Shanghai, China). The sequences were listed as follows:

DNA1: 5′-CTCTTCTCGACCGCC-3'

Hairpin A: 5′-GGGTAGGGCGGGTTGGGCCAGTCAGCGCCACGAACACATCGCTGACTGGCCCAACCCGCCCTACCCCGTGTTGAG-3′

GGCCCAACCCGCCCTACCCCGTGTTGAG-3'

Hairpin B: 5′-GGGTAGGGCGGGTTGGGCCAGTCAGCGCCACGAACACATCGCTGACTGGCCCAACCCGCCCTACCCGGCGCTGACTGG-3′

GCCCAACCCGCCCTACCCGGCGCTGACTGG-3'

2.2. Assay procedure

The purchased DNA is dissolved in 20 mM Tris-HAc buffer (20 mM Tris-HAc, 50 mM NaAc, 25 mM KAc, 10 mM $MgAc_2$, pH = 7.4) to prepare the DNA solution. The DNA solution was heated at 95 °C for 10 min, and gradually cooled to room temperature before use. Various concentrations of Hg^{2+} were incubated with the DNA1 (50 nM), hairpin A (200 nM), and hairpin B (400 nM) in 20 mM Tris-HAc buffer for 30 min at room temperature. 0.2 unit/μL of Exo III was introduced and incubated for 30 min. Then, 500 nM NMM was added to the above solution, and further incubated at room temperature for 30 min. The fluorescence spectra were recorded by the SpectraMax i3x (Molecular Devices, USA). The fluorescence intensity at 610 nm was used to estimate the performance of the proposed biosensor. To investigate the specificity of the assay, other metal ions including Pb^{2+},Cd^{2+}, Ag^+, Zn^{2+}, Mn^{2+}, Ni^{2+}, and Cu^{2+} at 10 nM were tested in the same way.

2.3. Native polyacrylamide gel electrophoresis (PAGE)

The hydrogel of 15% was prepared by mixing 5 mL 30% gel solution (29:1), 1 mL Tris-Borate-EDTA (TBE) buffer (10 ×), 100 μL ammonium persulfate (APS), 4 μL N,N,N′,N′- tetramethylethylenediamine (TEMED), and 3.8 mL H_2O. The gel was polymerized for 1.5 h at room temperature. After the gel is solidified, the comb is pulled out. The gel soaked in 1 × TBE buffer to pre-electrophoresis for 30 min at 30 V. Then, the loading sample which was subject to the 15% non-denaturing polyacrylamide gel electrophoresis (PAGE) was prepared by mixing 5 μL the resulting solution and 2 μL 6 × loading buffer. The PAGE was carried out in 1 × TBE at 70 V for 60 min. Finally, the PAGE gel was stained in diluted SYBR Green solution, and then scanned using a Gel Doc XR documentation system (Bio-RAD Laboratories Inc. USA).

3. Result and discussion

3.1. The strategy for Hg^{2+} monitoring

The design principle of the ultrasensitive and label-free fluorescence sensor for Hg^{2+} monitoring using G-quadruplex as the signal reporter is schematically illustrated in Scheme 1. The DNA1, hairpin A, hairpin B, and Exo III were used to construct the biosensor. There are five domains in hairpin A. Domain a is the 3′-protruding terminus. Domains b and c are the stem and loop parts of the probe, respectively. Domain d in hairpin A is to complementary to domain d' in hairpin B. Domain e is the caged G-rich sequence. The same domains of b, c, d, and e also appeared in hairpin B. In the presence of Hg^{2+}, DNA1 can bind with domain a *via* T-Hg^{2+}-T coordination chemistry to form the DNA1/hairpin A complex with a blunt 3′-terminus. Exo III then catalyze the stepwise removal of mononucleotides from this terminus, resulting in the release of DNA1 and the fragment containing domains c, d, and e. The released DNA1 can recycle and hybridize with other hairpin A probes to activate another round of hydrolysis reaction. The released fragment (domains c, d, and e) hybridized with hairpin B through base pairing to trigger Exo III-mediated digestion, thus, generating numerous free DNA sequences with the domains c, d, and e. After incubation with NMM and K^+, the domain e can fold into the G-quadruplex structure, which yields the high fluorescence intensity for output. Through the two-step circling amplification, the detection sensitivity can be significantly enhanced. In the absence of Hg^{2+}, the combination of domain a in hairpin A and the DNA1 is inhibited due to the T-T mismatches. Thus, the hairpin probes with the 3′-protruding terminus can be resistant to Exo III digestion. The G-rich sequence cannot be released, and the fluorescent signal is weak. Though this way, a strategy for the amplified detection of Hg^{2+} by the autocatalytic DNA circuit can be achieved.

3.2. Feasibility study

To verify the feasibility of this strategy, the fluorescence spectra of the Hg^{2+} sensor at different conditions were shown in Fig. 1A. In the presence of DNA1, two hairpin probes, and Exo III but no Hg^{2+}, the biosensor exhibited a negligible response (black curve), which implied that DNA1 could not bind with hairpin A without Hg^{2+}, so that G-rich sequence was not released to interact with the NMM. Noted that, when Hg^{2+}, Exo III, DNA1, and two hairpin probes were present in the sensing system, the fluorescence intensity dramatically increased (red curve), because DNA1 hybridizes with hairpin A *via* T-Hg^{2+}-T to promote Exo III digestion. Such high enhancement was attributed to the continuous cleavage process by Exo III, which can generate lots of free G-quadruplex structure. Then the G-quadruplex structure interacted with NMM to give out the improved signal. These results clearly demonstrated that this strategy can feasibly provide an amplified fluorescence signal for Hg^{2+} detection.

Polyacrylamide gel electrophoresis was used to confirm the results

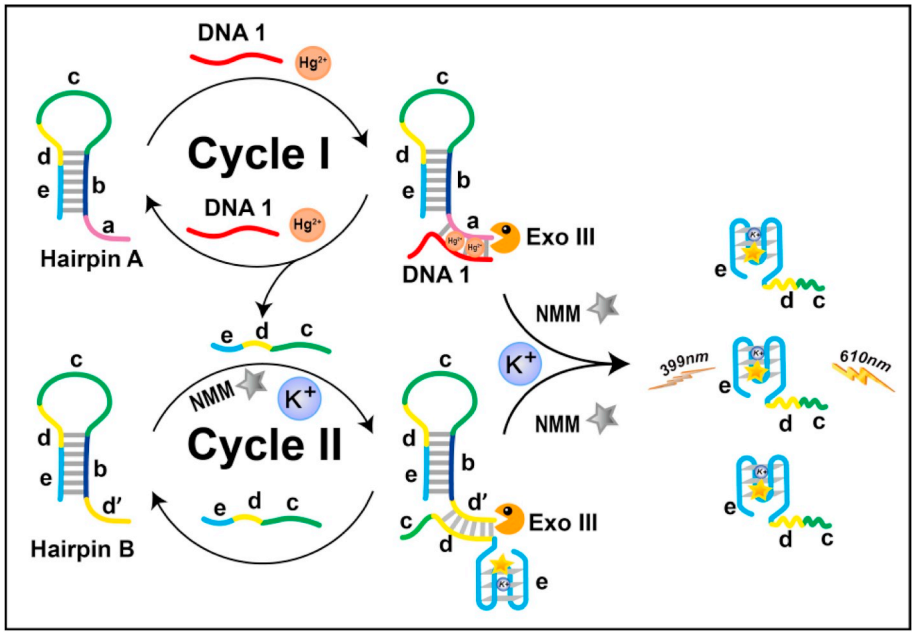

Scheme 1. Schematic illustration of the label-free fluorescence sensing platform for Hg^{2+} on the basis of Exo III-assisted cascade signal amplification using G-quadruplex as the signal report probe.

of the fluorescence assay. As shown in Fig. 1B, the band in lane 1 corresponded to the hairpin probes (A and B). When DNA1, hairpin A, and hairpin B co-existed in the system, two bands appear in lane 2, which corresponded to the hairpin probes (A and B) and DNA1, evidencing that in the absence of Hg^{2+}, signal amplification process will not happened. In the presence of Hg^{2+}, Exo III could cleavage the hairpin probes to generate the G-quadruplex structure (lane 3).

3.3. Optimization of assay conditions

The results of this experiment are affected by many conditions such as the concentration ratio of hairpin A to hairpin B, the temperature, the reaction time of Exo III, and the concentration of Exo III. These experimental conditions were optimized to achieve the best sensing performance.

In this study, the concentration ratio of hairpin A to hairpin B plays a critical role in the performance of the sensing system. Using a fixed concentration (200 nM) of hairpin A, the effect of concentration ratio of hairpin A to hairpin B on the response of the sensor was first investigated. As shown in Fig. S1 (Supporting Information), keeping constant conditions for other parameters, the signal-to-noise (S/N) ratio increased upon raising the concentration ratio of hairpin A to hairpin B from 1:1 to 1:2 and then decreased for further increasing the concentration ratio. The reason might be attributed to the fact that too much hairpin B could affect the binding kinetics between DNA1 and hairpin A, thus yielding a weak fluorescence signal. In order to obtain the best S/N ratio, the concentration ratio of hairpin A to hairpin B was selected as 1:2 for target detection.

The stability of the hairpin structure and the activity of Exo III were influenced by the reaction temperature of the system. Therefore, the effect of reaction temperature was also investigated by detecting 10 nM Hg^{2+} at different temperatures (4 °C, 25 °C, 37 °C, and 45 °C). The blank sample (in the absence of Hg^{2+}) was conducted at the same conditions. As shown in Fig. S2 (Supporting Information), in the presence of Hg^{2+}, the fluorescence signal increased with increasing temperatures in the range from 4 to 37 °C, but it decreased further increasing the temperatures (blue histogram). The background signal (green histogram) was elevated along with the increase in temperatures. The S/N ratio was the best when the reaction temperature was 25 °C. What leaded to the above results was that the structure of the hairpin probes could be destroyed with increased temperatures. Also the activity of Exo III may be deactivate. Therefore, 25 °C was chosen as the best reaction temperature.

The reaction time of Exo III is also an important factor affecting the signal amplification process. As displayed in Fig. S3 (Supporting Information), the fluorescence intensity of the solution containing 10 nM Hg^{2+} elevated gradually with the augment of reaction time within 30 min and tended to level off thereafter by controlling the reaction temperature at 25 °C, which indicated that the G-rich sequence was almost released from the hairpin probes to form G-quadruplexes. Thus, the optimum reaction time of Exo III is 30 min.

The effect of the concentration of Exo III on the response of the biosensor was also examined. As shown in Fig. S4 (Supporting Information), when the concentration of Exo III increased from 0.1 unit/μL to 0.2 unit/μL, the S/N level increased gradually. However, it decreased with further increasing the concentration. The cause of the above performance is that too many enzymes would cleave the hairpin probes even without the target, resulting a high background signal. Thus, 0.2 unit/μL Exo III was chosen for further experiments.

3.4. Analytical performance of the biosensor

A series of samples with different concentrations of Hg^{2+} were added to the reaction system to investigate the dynamic range and sensitivity of the assay under the optimal experimental conditions. As displayed in Fig. 2A, the fluorescence signal enhanced gradually along with the increase of the target concentration, indicating that more caged G-rich sequence were liberated from the hairpin probes. As shown in Fig. 2B, a proportional linearity between the fluorescence intensity and the logarithm of Hg^{2+} concentration was obtained in the range from 10 fM to 100 nM. The correlation equation can be expressed as follow: $F_{610} = 1.3 \times 10^5$ Lg C + 7.40×10^4 ($R^2 = 0.998$) where F_{610} was the fluorescence value at 610 nm and C represented the Hg^{2+} concentrations in the range from 10 fM to 100 nM. The limit of detection (LOD) is 10 fM. Compared with the previously reported method of Hg^{2+} detection, such as colorimetric sensor (the LOD was 10 pM) [6], electrochemical sensor (the LOD was 6.2 pM) [25], fluorescence sensor ((the LOD was 43 pM) [32], this sensing platform have higher

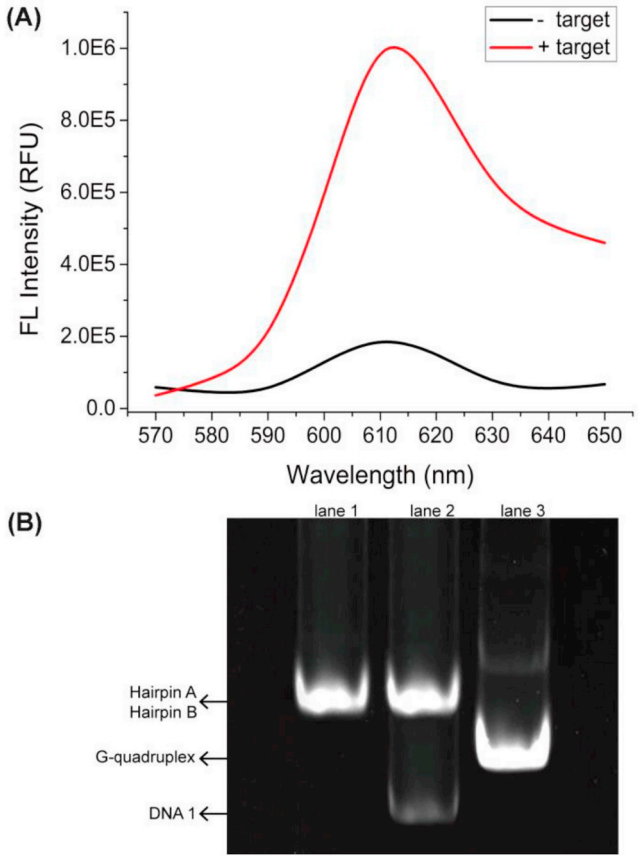

Fig. 1. (A) Feasibility of the label-free fluorescence sensing platform. Curve black: DNA1 (50 nM) + hairpin A (200 nM) + hairpin B (400 nM) + Exo III (0.2 unit/μL). Curve red: Hg^{2+} (10 nM) + DNA1 (50 nM) + hairpin A (200 nM) + hairpin B (400 nM) + Exo III (0.2 unit/μL). (B) The PAGE images of lane 1: hairpin A + hairpin B, lane 2: hairpin A + hairpin B + DNA1 + Exo III, lane 3: hairpin A + hairpin B + DNA1 + Exo III + Hg^{2+}. The experiments were performed at room temperature (25 °C). (For interpretation of the references to color in this figure legend, the reader is referred to the Web version of this article.)

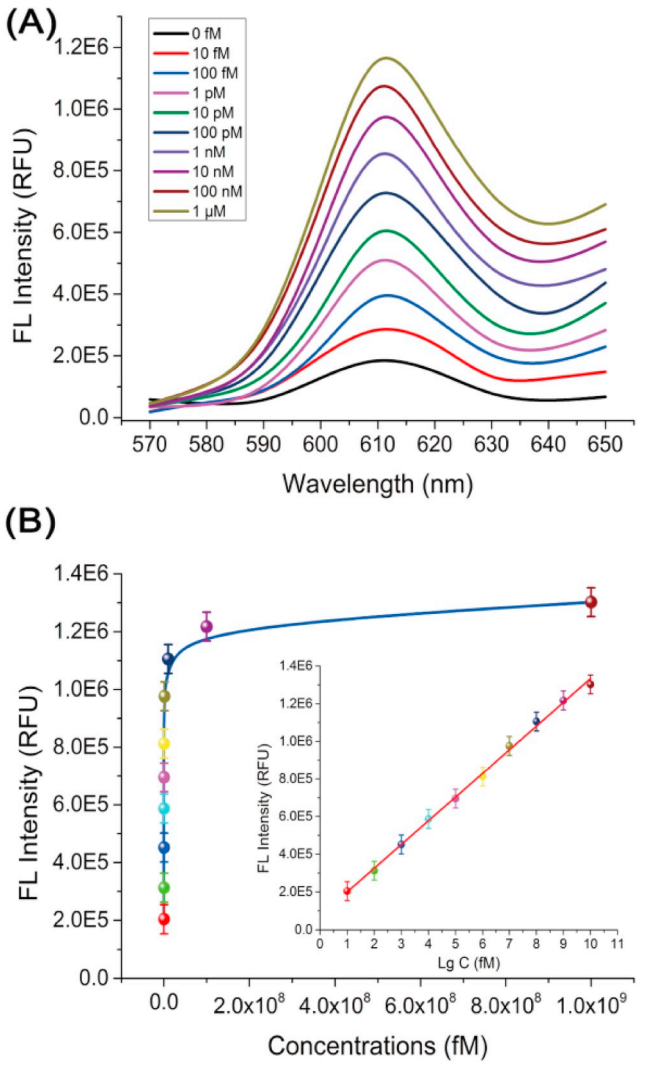

Fig. 2. (A) The fluorescence intensity of the label-free fluorescence sensing platform of various concentrations of Hg^{2+}. (B) Linear relationship between the fluorescence intensity and various concentrations of Hg^{2+}. The error bars denote the standard deviation of three independent measurements.

sensitivity, which could credit to the clever design of the hairpin probes and the integrating of Exo III-assisted target recycling onto the autocatalytic DNA machine to gather the cascade signal amplification. The strategy avoiding probe modification holds great promise for Hg^{2+} monitoring with high sensitivity.

To investigate the selectivity of this method, several other metal ions including Pb^{2+}, Cd^{2+}, Ag^{+}, Zn^{2+}, Mn^{2+}, Ni^{2+}, and Cu^{2+} at the same concentration of 10 nM were also performed by the present biosensor. As displayed in Fig. 3, only the sample with Hg^{2+} showed a significant fluorescence signal, while the samples with other metal ions displayed negligible fluorescence response compared with the blank sample, which demonstrated the high selectivity of our sensing system. Such high selectivity can be attributed to the specific T-Hg^{2+}-T coordination chemistry.

3.5. Real sample analysis

Real river water samples were tested to investigate the practical application of the biosensor. Different concentrations of Hg^{2+} (0.1, 10, 20, 40, and 50 nM) were added to the river water to detect the recovery. The results were showed in Table 1. The recovery and relative standard derivations (RSD) were in the range from 88% to 105% and 1.2%–6.4%, respectively, which indicated that the possible interference from the real water samples was negligible.

Moreover, the Hg^{2+} concentrations in tap water, lake water, and

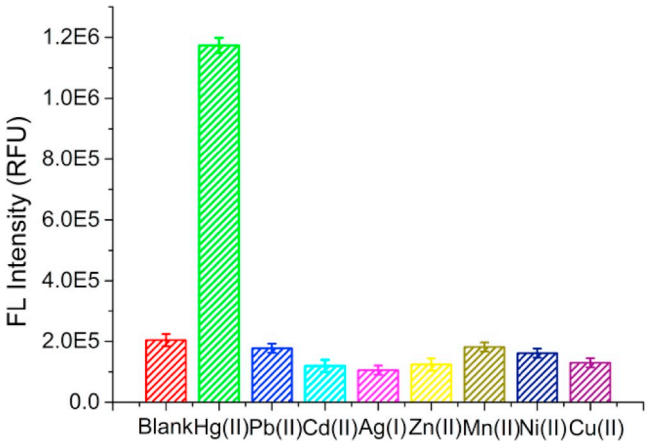

Fig. 3. The fluorescence intensity of different heavy metal ions. The concentration of all samples is 10 nM. The error bars denote the standard deviation of three independent measurements.

Table 1
Recovery experiments of Hg^{2+} determination in river water samples.

River water	Added (nM)	Found[a] (nM)	Recovery (%)	RSD (%)
1	0.1	0.088	88	6.4
2	10	10.5	105	1.2
3	20	20.5	103	3.8
4	40	39.6	99	1.8
5	50	49.3	98.6	3.8

[a] Mean of five determinations.

Table 2
Determination of Hg^{2+} in environmental water samples using the proposed biosensor and AFS.

Samples	AFS[a] (pM)	Proposed method[b] (pM)	Relative error (Re)[c] (%)
Tap water	82.5	79.6	−3.5
Lake water	145.6	147.8	1.5
Pond water	963.8	950.3	−1.4

[a] Each sample was analyzed using the standard AFS (atomic fluorescence spectrometer), and all values were obtained as an average of three repetitive determinations.
[b] Each sample was analyzed using our proposed biosensor, and all values were obtained as an average of three repetitive determinations.
[c] Our proposed method *vs*. AFS.

pond water were also validated by comparing to the standard AFS (atomic fluorescence spectrometer) analysis. The data revealed that no significant difference existed between the values measured using the proposed biosensor and the AFS method (see Table 2), confirming the accuracy of the developed sensor for Hg^{2+} detection.

4. Conclusions

In conclusion, an ultrasensitive and label-free autocatalytic DNA circuit for Hg^{2+} detection was successfully developed based on the ingeniously designed hairpin probes and Exo III by using G-quadruplex as the signal reporter. Firstly, we designed a DNA sequence and two hairpin probes. The DNA sequence can bind with hairpin A *via* T-Hg^{2+}-T to trigger the digestion reaction of Exo III. Then, the G-rich sequence was released, and hairpin B was used to cycle to amplify the signals by Exo III-assisted target recycling. Finally, due to the two-step circling signal amplifications, numerous G-quadruplex was released to interacted with NMM. So the detection sensitivity can be significantly enhanced with a detection limit of 10 fM. The assay exhibits excellent selectivity toward Hg^{2+} against other metal ions. Meanwhile, this method can be applied to the determination of Hg^{2+} in river water samples with satisfactory recovery. Additionally, The measurement procedure is carried out under isothermal conditions. To realize the detection of Hg^{2+}, DNA is used as the material for constructing the sensing platform. DNA is low cost, stable at both room temperature and higher temperatures, and easy to synthesize, which can be chosen as the ideal material to built biosensors. Also, the construction strategy herein is simple in design and economic in operation without labeling and immobilization procedures or separation and washing steps, making this fluorescent sensing system particularly suitable for routine monitoring of Hg^{2+} in environmental samples. We just need to mix the chemicals and stand for a while to get the detection results. The assay is cost-effective and each test costs approximately RMB 1 yuan. Therefore, the developed method herein is easy applied for routine monitoring of Hg^{2+} with its simple operation, excellent sensitivity and selectivity. With the above characteristics, the developed biosensor can be extended to be a universal sensing platform for other targets detection by substituting the target-recognition elements.

Conflicts of interest

There are no conflicts to declare.

Acknowledgements

Financial support was provided by the Key Projects in the National Science & Technology Pillar Program of China (Grant No. 2015BAD06B03).

Appendix A. Supplementary data

Supplementary data to this article can be found online at https://doi.org/10.1016/j.talanta.2019.120258.

References

[1] M. Zaib, M. Athar, A. Saeed, U. Farooq, Electrochemical determination of inorganic mercury and arsenic-A review, Biosens. Bioelectron. 74 (2015) 895–908.
[2] E.M. Nolan, S.J. Lippard, Tools and tactics for the optical detection of mercuric ion, Chem. Rev. 108 (2008) 3443–3480.
[3] Y. Zhang, M. Miro, S.D. Kolev, A novel on-line organic mercury digestion method combined with atomic fluorescence spectrometry for automatic mercury speciation, Talanta 189 (2018) 220–224.
[4] D. Zhang, S. Yang, H. Cheng, Y. Wang, J. Liu, Speciation of inorganic and organic species of mercury and arsenic in lotus root using high performance liquid chromatography with inductively coupled plasma mass spectrometric detection in one run, Talanta 199 (2019) 620–627.
[5] Y. Miyake, H. Togashi, M. Tashiro, H. Yamaguchi, S. Oda, M. Kudo, Y. Tanaka, Y. Kondo, R. Sawa, T. Fujimoto, T. Macchinami, A. Ono, MercuryII-mediated formation of thymine-HgII-thymine base pairs in DNA duplexes, J. Am. Chem. Soc. 128 (2006) 2172–2173.
[6] J. Chen, J. Pan, S. Chen, A naked-eye colorimetric sensor for Hg^{2+} monitoring with cascade signal amplification based on target-induced conjunction of split DNAzyme fragments, Chem. Commun. 53 (2017) 10224–10227.
[7] L. Li, Y. Wen, L. Xu, Q. Xu, S. Song, X. Zou, J. Yan, W. Zhang, G. Liu, Development of mercury (II) ion biosensors based on mercury-specific oligonucleotide probes, Biosens. Bioelectron. 75 (2016) 433–445.
[8] J. Liu, L. Liu, J. Chen, T. Wang, Y. Xu, Z. Dai, X. Zou, Selective and rapid detection of mercury ion based on DNA assembly and nicking endonuclease-assisted signal amplification, Anal. Methods 11 (2019) 3073–3078.
[9] F. Ma, Y. Chen, Y. Zhu, J. Liu, Electrogenerated chemiluminescence biosensor for detection of mercury (II) ion via target-triggered manipulation of DNA three-way junctions, Talanta 194 (2019) 114–118.
[10] X. Xue, F. Wang, X. Liu, One-step, room temperature, colorimetric detection of mercury (Hg^{2+}) using DNA/nanoparticle conjugates, J. Am. Chem. Soc. 130 (2008) 3244–3245.
[11] N. Dave, M.Y. Chan, P.J. Huang, B.D. Smith, J. Liu, Regenerable DNA-functionalized hydrogels for ultrasensitive, instrument-free mercury(II) detection and removal in water, J. Am. Chem. Soc. 132 (2010) 12668–12673.
[12] L. Ge, W. Wang, T. Hou, F. Li, A versatile immobilization-free photoelectrochemical biosensor for ultrasensitive detection of cancer biomarker based on enzyme-free cascaded quadratic amplification strategy, Biosens. Bioelectron. 77 (2016) 220–226.
[13] E. Lim, T.K. Kim, S. Paik, S. Haam, Y. Huh, K. Lee, Nanomaterials for theranostics: recent advances and future challenges, Chem. Rev. 115 (2015) 327–394.
[14] D.Y. Zhang, G. Seelig, Dynamic DNA nanotechnology using strand-displacement reactions, Nat. Chem. 3 (2011) 103–113.
[15] X. Chen, N. Briggs, J.R. McLain, A.D. Ellington, Stacking nonenzymatic circuits for high signal gain, Proc. Natl. Acad. Sci. U.S.A. 110 (2013) 5386–5391.
[16] L. Zeng, D. Zhou, J. Wu, C. Liu, J. Chen, A target-induced and equipment-free biosensor for amplified visual detection of pesticide acetamiprid with high sensitivity and selectivity, Anal. Methods 11 (2019) 1168–1173.
[17] H. Yu, J. Canoura, B. Guntupalli, O. Alkhamis, Y. Xiao, Sensitive detection of small-molecule targets using cooperative binding split aptamers and enzyme-assisted target recycling, Anal. Chem. 90 (2018) 1748–1758.
[18] W. Li, X. Liu, T. Hou, H. Li, F. Li, Ultrasensitive homogeneous electrochemical strategy for DNA methyltransferase activity assay based on autonomous exonuclease III-assisted isothermal cycling signal amplification, Biosens. Bioelectron. 70 (2015) 304–309.
[19] L. Zeng, D. Zhou, J. Gong, C. Liu, J. Chen, Highly sensitive aptasensor for trace arsenic(III) detection using DNAzyme as the biocatalytic amplifier, Anal. Chem. 91 (2019) 1724–1727.
[20] F. Xuan, X. Luo, I. Hsing, Ultrasensitive solution-phase electrochemical molecular beacon-based DNA detection with signal amplification by exonuclease III-assisted target recycling, Anal. Chem. 84 (2012) 5216–5220.
[21] Y. Chen, H.T.T. Duong, S. Wen, C. Mi, Y. Zhou, O. Shimoni, S.M. Valenzuela, D. Jin, Exonuclease III-assisted upconversion resonance energy transfer in a wash-free suspension DNA assay, Anal. Chem. 90 (2018) 663–668.
[22] X. Wang, X. Liu, T. Hou, W. Li, F. Li, Highly sensitive homogeneous electrochemical

assay for methyltransferase activity based on methylation-responsive exonuclease III-assisted signal amplification, Sens. Actuators B Chem. 208 (2015) 575–580.
[23] L. Lu, H. Su, F. Li, Ultrasensitive homogeneous electrochemical detection of transcription factor by coupled isothermal cleavage reaction and cycling amplification based on exonuclease III, Anal. Chem. 89 (2017) 8328–8334.
[24] J. Chen, S. Zhou, J. Wen, Disposable strip biosensor for visual detection of Hg_{2+} based on Hg_{2+}-triggered toehold binding and exonuclease III-assisted signal amplification, Anal. Chem. 86 (2014) 3108–3114.
[25] S. Wu, B. Zhang, F. Wang, Z. Mi, J. Sun, Heating enhanced sensitive and selective electrochemical detection of Hg^{2+} based on T-Hg^{2+}-T structure and exonuclease III-assisted target recycling amplification strategy at heated gold disk electrode, Biosens. Bioelectron. 104 (2018) 145–151.
[26] J.T. Davis, G-quartets 40 years later: from 5'-GMP to molecular biology and supramolecular chemistry, Angew. Chem. Int. Ed. 43 (2004) 668–698.
[27] Y. Sannohe, M. Endo, Y. Katsuda, K. Hidaka, H. Sugiyama, Visualization of dynamic conformational switching of the G-quadruplex in a DNA nanostructure, J. Am. Chem. Soc. 132 (2010) 16311–16313.
[28] J. Chen, S. Chen, F. Li, Instrument-free visual detection of tetracycline on an autocatalytic DNA machine using a caged G-quadruplex as the signal reporter, Chem. Commun. 53 (2017) 8743–8746.
[29] J. Mergny, D. Sen, DNA quadruple helices in nanotechnology, Chem. Rev. 119 (2019) 6290–6325.
[30] P. Chen, K. Huang, P. Zhang, E. Sawyer, Z. Wu, X. Wei, B. Ying, J. Geng, Exonuclease III-assisted strand displacement reaction-driven cyclic generation of G-quadruplex strategy for homogeneous fluorescent detection of melamine, Talanta 203 (2019) 255–260.
[31] Q. Li, Z. Liu, D. Zhou, J. Pan, C. Liu, J. Chen, A cascade toehold-mediated strand displacement strategy for label-free and sensitive non-enzymatic recycling amplification detection of the HIV-1 gene, Analyst 144 (2019) 2173–2178.
[32] Y. Jiang, Q. Duan, G. Zheng, L. Yang, J. Zhang, Y. Wang, H. Zhang, J. He, H. Sun, D. Ho, An ultrasensitive and ratiometric fluorescent probe based on the DTBET process for Hg^{2+} detection and imaging applications, Analyst 144 (2019) 1353–1360.